

Soil moisture as an indicator of growing-season herbaceous fuel moisture and curing rate in grasslands

Sonisa Sharma^{A,D}, J. D. Carlson^B, Erik S. Krueger^A, David M. Engle^C, Dirac Twidwell^{C,E}, Samuel D. Fuhlendorf^C, Andres Patrignani^{A,F}, Lei Feng^{A,G} and Tyson E. Ochsner^{A,H}

^ADepartment of Plant and Soil Sciences, Oklahoma State University, Stillwater, OK 74078, USA.

^BDepartment of Biosystems and Agricultural Engineering, Oklahoma State University, Stillwater, OK 74078, USA.

^CDepartment of Natural Resources Ecology and Management, Oklahoma State University, Stillwater, OK 74078, USA.

^DPresent address: Division of Plant Biology, Noble Research Institute, Ardmore, OK 73401, USA.

^EPresent address: Department of Agronomy and Horticulture, University of Nebraska – Lincoln, Lincoln, NE 68588, USA.

^FPresent address: Department of Agronomy, Kansas State University, Manhattan, KS 66506, USA.

^GPresent address: College of Information and Electrical Engineering, China Agricultural University, Beijing, 100083, China.

^HCorresponding author. Email: tyson.ochsner@okstate.edu

Abstract. Soil moisture depletion during the growing season can induce plant water stress, thereby driving declines in grassland fuel moisture and accelerating curing. These drying and curing dynamics and their dependencies on soil moisture are inadequately represented in fire danger models. To elucidate these relationships, grassland fuelbed characteristics and soil moisture were monitored in nine patches of tallgrass prairie under patch-burn management in Oklahoma, USA, during two growing seasons. This study period included a severe drought (in 2012), which resulted in a large wildfire outbreak near the study site. Fuel moisture of the mixed live and dead herbaceous fuels (MFM) clearly tracked soil moisture, expressed as fraction of available water capacity (FAW). MFM decreased with decreasing soil moisture below an FAW threshold of 0.59 and fell below 30% only when FAW fell below 0.30. Likewise, the curing rate increased linearly as FAW declined below 0.30, while Normalized Difference Vegetation Index (NDVI) readings failed to adequately respond to rapid drying and curing of the fuelbed. Incorporating soil moisture observations into grassland fuelbed models could result in more accurate fuel moisture and curing estimates, contributing to improved wildfire danger assessments and reduced losses of life and property due to wildfire outbreaks.

Keywords: curing, drought, fuel moisture, grassland, herbaceous, NDVI, soil moisture, wildfire.

Received 19 November 2019, accepted 17 September 2020, published online 16 October 2020

Introduction

Fire is an integral part of grassland ecosystems worldwide and can, in certain contexts, increase biodiversity (Deák *et al.* 2014) and improve the performance of grazing livestock (Limb *et al.* 2011). However, wildfires also increase greenhouse gas emissions and cause major economic losses to society worldwide (Yebra *et al.* 2008). For example, the National Interagency Fire Center (NIFC) reported that federal firefighting expenditures in the US exceeded US\$2.9 billion in 2017 (NIFC 2017). Savanna and grassland wildfires are particularly widespread, accounting for approximately 90% of the global area burned over the last century (Mouillot and Field 2005). These grassland wildfires can be large and devastating. For example, the North-west

Oklahoma Complex Fires, the largest recorded wildfire complex ever originating in the state of Oklahoma, USA, burned over 315 000 ha of grassland across Oklahoma and Kansas during 6–24 March 2017 (NIFC 2017). Reducing the harmful impacts of such wildfires and saving lives requires improved fire danger assessments (Yebra *et al.* 2013). Current fire danger models have a limited ability to anticipate grassland wildfires when drought causes fuel curing, the transition of live herbaceous vegetation to dead. One approach to improving fire danger models is through better prediction of change in grassland fuelbed characteristics.

Live fuel moisture (LFM), the water content of live fuels expressed as a percentage of the oven-dry weight, is a key input

variable in many models of fire behaviour, such as the dynamic fuel models of Scott and Burgan (2005) developed for use with Rothermel's fire spread model (Rothermel 1972). Fuel moisture is also a key variable in physics-based models such as the Wildland–Urban Interface Fire Dynamics Simulator (Mell *et al.* 2010; Overholt *et al.* 2014) and FIRETEC (Linn *et al.* 2002; Marino *et al.* 2012). However, direct measurement of LFM in grassland fuelbeds is laborious and time-consuming, requiring destructive biomass sampling, separation by hand of live and dead fuels, and oven-drying and weighing of samples. Tracking change in grassland LFM also requires repeated sampling during periods when environmental conditions are changing. Few agencies or fire practitioners have the resources necessary for this level of intensive direct sampling, which is one reason why fire danger assessments often use proxy estimates of LFM derived from weather-based indices (e.g. Keetch–Byram Drought Index) or satellite remote sensing (e.g. Moderate Resolution Imaging Spectroradiometer – MODIS, Visible Infrared Imaging Radiometer Suite – VIIRS) (Dennison *et al.* 2008; García *et al.* 2008; Yebra *et al.* 2013). Moreover, grassland prescribed burn managers rarely incorporate LFM into fire prescriptions (Twidwell *et al.* 2016).

Curing, the transition of herbaceous fuel from live to dead, is a primary controlling variable of grassland fire dynamics (Kidnie *et al.* 2015). The degree of curing is defined as the ratio of dead herbaceous fuel mass to the total herbaceous fuel mass and is generally expressed as a percentage. The degree of curing is a key input in the systems used for fire danger ratings and rate of fire spread predictions in Australia and Canada (Noble *et al.* 1980; Cheney *et al.* 1998; Wotton *et al.* 2009). As with LFM measurement, direct measurements of degree of curing require time-consuming manual separation of live and dead fuels. Therefore, in practice, degree of curing is more commonly determined by visual estimation (Newnham *et al.* 2011).

Soil moisture metrics have been recently proposed as proxies capable of reflecting variability in temporally dynamic herbaceous fuel moistures and curing rates in grassland fuelbeds (Kidnie *et al.* 2015; Krueger *et al.* 2016). These possibilities have been facilitated by the development of numerous soil moisture monitoring networks at the regional scale, e.g. the Oklahoma Mesonet, West Texas Mesonet and Tibetan Plateau Observatory, and at the national scale, e.g. the USDA Natural Resources Conservation Service Soil Climate Analysis Network (SCAN), NOAA Climate Reference Network (CRN) and the OzNet hydrological monitoring network in Australia (Ochsner *et al.* 2013). Globally available, satellite-based soil moisture products, such as those produced by NASA's Soil Moisture Active Passive (SMAP) mission and the European Space Agency's Soil Moisture Ocean Salinity (SMOS) mission, also provide new opportunities to use soil moisture data to estimate fuel moisture and curing levels.

A previously reported strong relationship between soil moisture, in the form of fraction of available water capacity (FAW), and sizes of growing-season wildfires in Oklahoma, USA, provided indirect evidence that soil moisture influences fuel moisture and grass curing during the growing season (Krueger *et al.* 2015). Soil moisture also played a major role in predicting the probability of large growing-season wildfires in Oklahoma (Krueger *et al.* 2016) and across the contiguous US (Jensen *et al.*

2018). The results of these US studies have recently been supported by a global analysis based on remotely sensed soil moisture data, showing that soil moisture anomalies continuously decrease in the months leading up to wildfire occurrences (O *et al.* 2020). The key missing link in all these studies is direct collocated measurements of the dynamics of soil moisture and fuelbed characteristics.

In the present study, our overall objective was to assess the potential for the soil moisture metric FAW to serve as an indicator of fuel moisture and curing level in the growing season for grassland fuelbeds dominated by warm-season grasses. Our specific objectives were: (i) to quantify the temporal dynamics of grassland fuel moisture and FAW; (ii) to describe the relationship between fuel moisture and FAW; and (iii) to determine the relationships between rate and degree of curing and FAW. Quantitative understanding of these relationships would be an important new contribution to fire research and a necessary foundation for the subsequent inclusion of soil moisture data in fire behaviour models, which could improve fire danger assessments.

Materials and methods

Study site

This research was conducted at the Oklahoma State University Range Research Station (latitude 36.06°, longitude –97.22°, 300 m above sea level) located near Stillwater, Oklahoma, USA. The location is primarily tallgrass prairie dominated by warm-season grasses. Major vegetation species include little bluestem (*Schizachyrium scoparium* (Michx.) Nash), big bluestem (*Andropogon gerardii* Vitman), Indiangrass (*Sorghastrum nutans* (L.) Nash) and scattered trees including post oak (*Quercus stellata* Wangenh.) and eastern redcedar (*Juniperus virginiana* L.). The predominant soils at this site include the Grainola series (fine, mixed, thermic Vertic Haplustalf) covering ~60% of the area, and the Coyle series (fine loamy, siliceous, thermic Udic Argiustoll) covering ~35% of the area (Gillen *et al.* 1990). The study site consisted of three pastures ranging in size from 50 to 63 ha, with each pasture subdivided into six approximately equal-sized unfenced patches, identified by the numbers 1 through 6. These patches were used to apply a patch burning treatment designed to increase ecological heterogeneity while preventing woody plant encroachment (Fuhlendorf and Engle 2004). Each year, two of the six patches were burned: one during the late dormant season (February–April) and one during the late growing season (July–October). Patches were burned every 3 years to represent different successional stages (Fuhlendorf and Engle 2004). The patch burning sequence has been continuous since the pastures were established in 1999. In the present study, sampling occurred in the three patches in each pasture that were burned during the growing season. These nine patches (numbered 1, 3 and 5 in each pasture) were burned respectively during the following dates: Patches 1, 20–21 October 2011; Patches 3, 13–14 July 2009 and 20 September, 15 October, 31 October 2012; and Patches 5, 10–11 July 2010 and 24–25 October 2013. Each pasture was grazed by cattle at a moderate stocking rate across burned and unburned patches. During the timeline of our study, a major drought occurred at this study site (Bielski *et al.* 2018) that

provided an opportunity to study a wide range of herbaceous fuel moistures and grass curing rates and their relationship with changes in soil moisture. That drought created conditions of elevated fire danger and contributed to a large growing-season wildfire outbreak near the study site during August 2012.

Terminology

There is some lack of clarity in the literature about which herbaceous fuels are considered 'live' at any moment and exactly how to objectively separate and measure the live and dead herbaceous fuels. It is also difficult to define and to operationally determine when herbaceous fuel is 'dead', and representing these fuels as either live or dead may be too simplistic for fire behaviour prediction (Kidnie *et al.* 2015). Visual estimation of live and dead fuels in the field is highly subjective and manual separation is prohibitively time-consuming for studies of fuelbed dynamics when, as in the case of the present study, thousands of samples are required.

To provide greater conceptual and operational clarity for fuelbed descriptions, Kidnie *et al.* (2015) proposed and defined the following fuel categories: (1) old dead; (2) new dead; (3) senescing; and (4) green. Dead fuels are those appearing light to dark brown or grey with no remaining green chlorophyll pigment and stalks that break easily. Green fuels are green in colour and show no obvious signs of tissue deterioration or aging. The leaves are typically soft and the stalks typically show visible moisture if crushed or broken. Senescing fuels are in transition between these two states, and green, senescing and dead tissues may be present simultaneously in a single plant. In this study, we focused on the moisture of the mixed live and dead herbaceous fuels (MFM), which can include all four categories of Kidnie *et al.* (2015), as well as on dead fuel moisture (DFM, old dead and new dead together) and green fuel moisture (GFM), because only these categories can be objectively measured without manual separation of bulk samples containing both live and dead fuels.

Data collection and calculations

GFM, MFM, DFM and Normalized Difference Vegetation Index (NDVI) were measured by field sampling every 2 weeks in each patch during the growing seasons (1 May to 31 October) of 2012 and 2013. In each of the nine patches during each sampling period, 12 vegetation samples (a mix of live and dead fuels) were obtained by clipping herbaceous vegetation to a 2-cm stubble height within randomly selected 0.25-m² quadrats along a transect spanning the patch. These 'mixed' samples were weighed in the field and later weighed after drying at 70°C for 48 h. To account for variability in fuel loads between the 12 sampling locations in each patch, the fuel moisture values of the mixed samples were averaged on a mass-weighted basis, such that quadrats containing a greater fuel mass received more weight in the calculation. This mass-weighted mean of the MFM from the 12 mixed-fuel samples was used to represent MFM for each patch and sampling period. In addition, six samples each of ~100 g field (wet) weight of pure green and pure dead herbaceous fuel were hand-plucked, weighed in the field, oven-dried and weighed again to determine GFM and DFM for each patch and sampling period. The arithmetic means of the six measurements of green and dead fuel moisture were then used to represent GFM and DFM in that patch for that sampling period.

Determining the rate of curing (i.e. the rate at which fuels transition from live to dead) requires estimates of the mass of live and dead fuels for each sampling period. Following Kidnie *et al.* (2015), 'live' in this context includes both green and senescing fuels. As we did not manually separate live and dead fuels, our approach adapts the constituent differential method (CDM) developed by Gillen and Tate (1993), which built on the earlier work of Cooper *et al.* (1957). The CDM equations allow estimation of live and dead fuel loads using inputs of mixed fuel load, MFM, DFM and LFM; their derivation can be found in the supplementary material. The mass of live fuel (m_L), i.e. the live fuel load, for each patch and sampling time was estimated by:

$$m_L = m_M \frac{\text{MFM} - \text{DFM}}{\text{LFM} - \text{DFM}} \quad (1)$$

where m_M is the patch average mass of mixed fuel (g m⁻²), i.e. the total mixed-fuel load, and LFM is the live fuel moisture, for which the estimation procedure will be described below. The mass of dead fuel (m_D), i.e. the dead fuel load for each patch and sampling time was estimated by:

$$m_D = m_M - m_L \quad (2)$$

The curing rate (CR, g m⁻² d⁻¹) between two consecutive sampling times t_1 and t_2 , between which m_L decreased and m_D increased, was calculated by:

$$\text{CR} = \frac{m_L(t_1) - m_L(t_2)}{t_2 - t_1} \quad (3)$$

The CDM was used wherever possible on the patch scale to estimate the live and dead fuel loads. In some cases, however, needed input data for the CDM were missing, and it was not possible to calculate live and dead fuel loads. In some other cases, herbaceous fuels were, by visual assessment, counted as either 100% live (e.g. with regrowth in a recently burned patch) or 100% dead (e.g. after a killing freeze when all plants were dormant and aboveground herbaceous vegetation was dead).

Applying Eqns 1 and 2 requires estimates of LFM, which we did not directly measure. Under the sampling protocol established for this study (no recent rain or dew), dead herbaceous fuels at sampling time had lower fuel moisture values than those of mixed fuels, which had lower fuel moisture than green fuels. Senescing fuels had values intermediate between those of the mixed and green fuels. Therefore, $\text{DFM} \leq \text{MFM} \leq \text{LFM} \leq \text{GFM}$. Based on this relationship, we estimated three possible values for LFM based on our measurements of MFM and GFM using the following equations:

$$\text{LFM}_3 = \text{GFM} \quad (4)$$

$$\text{LFM}_2 = \text{MFM} + \frac{2}{3}(\text{GFM} - \text{MFM}) \quad (5)$$

$$\text{LFM}_1 = \text{MFM} + \frac{1}{3}(\text{GFM} - \text{MFM}) \quad (6)$$

We did not include an estimate based on the assumption that LFM = MFM because that would result in all fuel being categorised as live, which would be incorrect in most cases. For each patch and sampling period, we used the three LFM values of Eqns 4–6 in Eqn 1 to obtain three estimates of live fuel load, each of which were then used in Eqn 3 to obtain three estimates of the curing rate. Likewise, we obtained three estimates of dead fuel load for each patch and sampling date.

Because indices based on remote sensing of vegetation have often been used to represent grassland curing (e.g. Newnham *et al.* 2011), canopy reflectance was measured at each sampling location before clipping. Reflectance was measured using a hand-held multispectral radiometer (MSR5R, Cropscan, Inc.) 2 m above ground between 1200 and 1700 hours. The radiometer was calibrated using a two-point upward and downward calibration procedure on a clear-sky day each season before sampling began, as recommended by the manufacturer. The radiometer measured percentage reflectance in five bands in the 460–1750 nm region (approximate centre wavelengths 485, 560, 660, 830 and 1650 nm). NDVI was calculated for each sampling location on the basis of the reflectance at wavelengths of 660 and 830 nm (Rouse *et al.* 1974) and these individual NDVI values were averaged for each patch and sampling period. NDVI is a commonly used surrogate for vegetation curing (Allan *et al.* 2003), and it is an important predictor for estimating fuel moisture content and biomass in grasslands (Sharma *et al.* 2018).

Soil moisture in the form of volumetric water content was measured hourly at four depths (5, 10, 20 and 50 cm) in each patch using reflectometry-based sensors (Model 655, Campbell Scientific). The soil moisture sensors were calibrated using Coyle–Lucien complex soil obtained from one of the patches on 13 March 2013. The calibration equation was

$$\theta = 0.107\sqrt{K_a} - 0.119\sqrt{EC} - 0.105 \quad (7)$$

where θ is the volumetric water content ($\text{cm}^3 \text{cm}^{-3}$), K_a is the apparent dielectric permittivity reported by the sensor (unitless), and EC is the bulk electrical conductivity of the soil reported by the sensor (dS m^{-1}). This equation provided a root-mean-squared error of $0.03 \text{ cm}^3 \text{cm}^{-3}$ on the calibration dataset consisting of soils from the 10-, 20- and 50-cm depths, with volumetric water contents ranging from 0 to $0.52 \text{ cm}^3 \text{cm}^{-3}$, EC values ranging from 0 to 3.09 dS m^{-1} , and soil temperatures ranging from 10 to 40°C .

FAW was calculated based on the daily-averaged volumetric water content and the soil water retention properties for each patch and depth. The field capacity for each patch and depth was estimated as the soil water content retained by samples equilibrated at -10 kPa in laboratory pressure cells. The field capacity values ranged from 0.22 to $0.37 \text{ cm}^3 \text{cm}^{-3}$. The permanent wilting point for each patch and depth was estimated as the soil water content retained by samples equilibrated at -1500 kPa in a laboratory pressure plate apparatus. The permanent wilting point values ranged from 0.05 to $0.28 \text{ cm}^3 \text{cm}^{-3}$.

The available water capacity for each patch and depth was calculated as the difference between field capacity and permanent wilting point. Plant available water for each day, patch and depth was calculated as the difference between the measured

volumetric water content and the permanent wilting point. Available water capacity and plant available water were: (1) linearly interpolated between measurement depths; (2) linearly extrapolated for the 0–5-cm layer; and (3) integrated across the 0–40-cm layer by trapezoidal numerical integration using the *trapz* function in *Matlab R 2018a* (Mathworks 2018). FAW for the 0–40-cm layer was then calculated as the ratio of the plant available water to the available water capacity. Values of FAW are typically between 0 (no plant available water) and 1 (soil at field capacity). Values of FAW less than 0.5 often indicate conditions of plant water stress (Allen *et al.* 1998).

To provide climatological context, reference evapotranspiration (ET_0) was calculated using the Food and Agriculture Organization FAO-56 method (Allen *et al.* 1998) based on daily weather data from the Marena station of the Oklahoma Mesonet (McPherson *et al.* 2007). That station is located only 200 m from one of the three pastures in the present study. Weather data included maximum and minimum air temperature ($^\circ\text{C}$), minimum and maximum relative humidity (%), average wind speed (m s^{-1}), precipitation (mm) and solar radiation (W m^{-2}).

Data analysis

Because the patch burning treatment can dramatically alter fuelbed properties, the vegetation and soil moisture data were averaged across pastures for each level of time since fire. For each growing season, there were three patches in their first year since fire, three in their second year, and three in their third year. The time series of FAW and of fuel moisture for the green, mixed and dead fuel categories were plotted to visualise their seasonal dynamics. The relationships between fuel moisture for each fuel category and FAW were assessed using box-and-whisker plots with fuel moisture categories of 0–30%, >30–120%, and >120%, which are the categories in the dynamic fuel model of Scott and Burgan (2005). That model considers fuels as ‘fully cured’ when the herbaceous moisture content is 30% or less (all live fuel has been converted to dead fuel) and ‘uncured’ when the live herbaceous moisture content is $\geq 120\%$. Fuels with intermediate live moisture contents are considered ‘partially cured’ in that model.

To describe the relationships between FAW and the rate of grass curing, the CRs for each sampling interval in which the estimated live fuel load decreased and dead fuel load increased were plotted against the average FAW for that interval. Visual inspection of the data suggested that a soil moisture threshold existed below which CR is driven by FAW and above which FAW and CR are unrelated. This threshold was identified using piecewise linear regression:

$$\begin{cases} \text{CR} = b_1 + m_1 \times \text{FAW}, & \text{for FAW} \leq \text{FAW}_{\text{bp}} \\ \text{CR} = b_1 + \text{FAW}_{\text{bp}}(m_1 - m_2) + m_2 \times \text{FAW}, & \text{for FAW} > \text{FAW}_{\text{bp}} \end{cases} \quad (8)$$

where b_1 is the intercept, m_1 is the slope of the first segment, m_2 is the slope of the second segment, and FAW_{bp} is the breakpoint between segments. The breakpoint was identified using the *Matlab R 2018a* (Mathworks 2018) *fitnlm* function and the Levenberg–Marquardt non-linear least-squares algorithm (Seber and Wild 2003).

As with CR, preliminary analyses of the FAW–MFM relationship also suggested a threshold soil moisture value below which MFM was strongly related to FAW. Therefore, this relationship was also described using Eqn 8, substituting MFM for CR, and using data from sampling intervals in the growing season when the soil moisture was declining. For both CR and MFM, we found that relationships with FAW were not significant above their respective thresholds. Therefore, results are presented for reduced models reflecting a slope of zero above the identified breakpoints (i.e. $m_2 = 0$).

Because NDVI measurements are often used as a surrogate for the cumulative degree of curing, we plotted NDVI as a function of FAW for every sampling interval in the growing season when the soil moisture was declining. The relationship between FAW and NDVI was represented mathematically using a logistic equation (Chen and Chang 1991; Zhang *et al.* 2017).

$$\text{NDVI} = \frac{a}{1 + \exp[(b - \text{FAW}) \times c]} + d \quad (9)$$

where a is a parameter representing the range of NDVI values, b is a parameter indicating the inflection point of the curve, the parameter c defines the slope of the relationship, and d is a parameter representing the minimum NDVI values. Representing the relationship in this way allowed us to quantitatively determine the critical value of FAW below which NDVI declines, i.e. the value at which the greenness of the fuelbed begins to decrease. That critical value is given by:

$$\text{FAW}_{\text{crit}} = b - \frac{\ln\left(\frac{a}{0.95-d} - 1\right)}{c} \quad (10)$$

Here, FAW_{crit} is the value of FAW at which NDVI falls to 95% of the value of the upper asymptote. All analyses were conducted with *Matlab R 2018a* (Mathworks 2018).

Results

Precipitation and reference evapotranspiration (ET_0)

Above-average early growing-season precipitation in 2012 gave way to below-average precipitation throughout that summer, whereas precipitation was near average for most of 2013 (Fig. 1). In 2012, cumulative precipitation was ~ 50 mm (25%) above average by the end of April, creating favourable conditions for early-season vegetative growth. However, below-average rainfall during May 2012 resulted in cumulative precipitation returning to average by the start of June. A substantial precipitation deficit began developing in late June, and the deficit reached 150 mm (23%) below average by early August before abating slightly in late August. By the end of 2012, the cumulative precipitation was ~ 300 mm (33%) below average. In contrast, at the end of 2013, the cumulative precipitation was near average, i.e. ~ 900 mm. As described in detail below, the precipitation dynamics were reflected in the soil moisture levels, with FAW indicating adequate soil moisture during most of the 2013 growing season but severe or extreme drought during most of July–October 2012.

High temperatures in 2012 contributed to relatively high ET_0 values that year, whereas ET_0 was slightly below average for

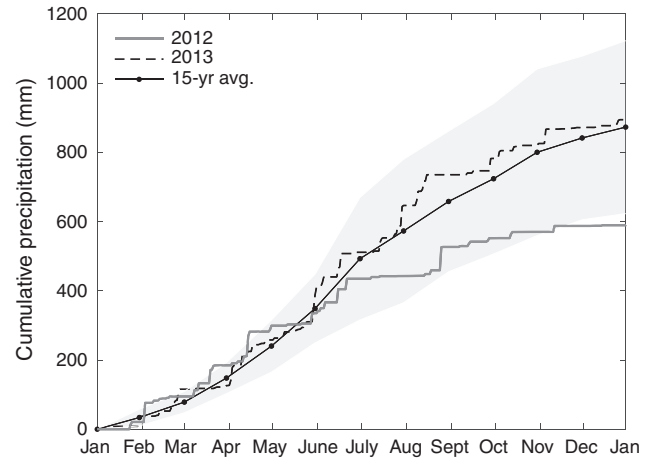


Fig. 1. Cumulative precipitation for 2012 and 2013 at the Marena station of the Oklahoma Mesonet along with the 15-year average (1999–2013) of monthly cumulative precipitation for the site. The shaded area represents 1 s.d. above and below the average.

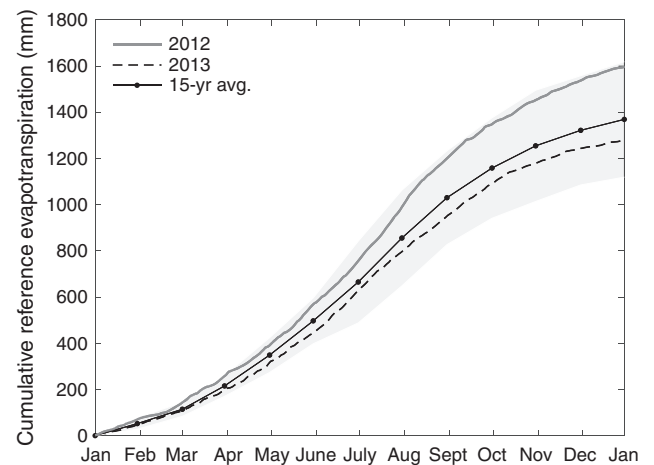


Fig. 2. Cumulative reference evapotranspiration (ET_0) for 2012 and 2013 at the Marena station of Oklahoma Mesonet along with the 15-year average (1999–2013) of monthly cumulative ET_0 for the site. The shaded area represents 1 s.d. above and below the average.

most of 2013 (Fig. 2). The cumulative ET_0 in 2012 was ~ 50 mm above average by early May and increased to >200 mm above average by the end of the year. In contrast, cumulative ET_0 in 2013 was near average through June and ~ 100 mm below average by the end of the year. The cumulative atmospheric water deficit ($ET_0 - \text{precipitation}$) reached ~ 900 mm by the end of the 2012 growing season and ~ 375 mm by the end of the 2013 growing season. The 15-year average of cumulative atmospheric water deficit at the end of the growing season for this site is ~ 525 mm, so the drought conditions that developed during the 2012 growing season were severe. That severity was reflected by the US Drought Monitor, which indicated extreme to exceptional drought conditions for the study area beginning on 24 July and extending through to the end of the 2012 growing season.

Soil moisture, fuel moisture and wildfire activity

The contrasting weather conditions between the two growing seasons were reflected in soil moisture levels. FAW typically ranges between 0 (no plant available water) and 1 (soil at field capacity), with values less than 0.5 often associated with plant water stress (Allen *et al.* 1998). For a given sampling date, the spatial variability of FAW was relatively low, with the standard deviation of FAW averaging 0.08 across pastures and 0.07 across patches. During 2012, FAW indicated near-constant conditions of soil moisture stress, with most values ranging from 0.2 to 0.6. The initial FAW measurements that growing season were <0.6 on 22 May 2012, reached a maximum value of 0.67 on 5 June 2012, and then declined steadily until 14 August 2012 as drought conditions developed (Fig. 3a). By 20 June 2012, FAW fell below 0.5, with FAW reaching a minimum of <0.2 during August, indicative of extreme drought conditions (Sridhar *et al.* 2008).

A large wildfire outbreak occurred in Payne County, Oklahoma, the county in which this study was located, during 3–5 August 2012. The dashed vertical line in Fig. 3 indicates 3 August 2012. These fires burned >11 000 ha in Payne County and bordering areas. The largest growing-season wildfire in Oklahoma that summer, the Freedom Hill Fire, ignited on 2 August, burning >23 600 ha, and was located just east of Payne County, ~70 km from the study site, making for a total of over 34 600 ha burned in the vicinity of the study site during early August 2012.

After rainfall totalling 67 mm between 25 August and 26 August, FAW briefly increased to >0.5 on 29 August 2012, but dropped again to <0.3 by 12 September 2012, and remained low for the rest of the growing season. In contrast to 2012, FAW was often greater than the threshold for soil moisture stress in 2013. FAW reached maximum values above 0.9 on 11 June 2013 and did not drop below 0.5 until 8 July 2013, 18 days later than in 2012. Rainfall increased FAW through July and August 2013, with values topping 0.6 in August, well above the average for that time of year (Krueger *et al.* 2016). However, dry conditions in September caused a secondary decline in FAW, reaching a minimum of 0.17 on 16 September 2013 (Fig. 3b). Wildfire conditions (i.e. low humidity, high air temperature, high wind speed) did not occur in Payne County in late September 2013, and neither did large wildfires.

In 2012, the maximum GFM of 206% was recorded on the first sampling date, 24 May (Fig. 3c). GFM dropped steeply between the second and third sampling dates, coincident with the onset of decreasing soil moisture levels. The minimum recorded GFM values of <100% occurred during the first half of August 2012, coincident with the minimum FAW values of <0.2. GFM then increased above 100% in response to precipitation in late August and remained above 100% for the rest of the growing season.

As in 2012, the maximum GFM in 2013 was recorded on the first sampling date of the growing season (13 May 2013), but GFM was considerably higher than at the same time the previous year (879% *v.* 206%; possible explanations for these exceptionally high GFM values in May 2013 are considered in the Discussion section). GFM declined as the season progressed until stabilising at values of ~200% through July and August

2013, and GFM never fell below 100% in 2013. The minimum GFM was 128% on 19 October 2013 as the vegetation senesced at the end of growing season (Fig. 3d). The patches burned in September–October 2012 (Patches 3) had much lower GFM values than the other patches in May–June of 2013. The patch burn in 2012 removed virtually all the dead herbaceous fuels from those patches, and all the new growth was classified as green fuel.

Above-average rainfall and warmer than average temperatures produced rapid early growth in 2012, with moisture of the mixed live and dead herbaceous fuels (MFM) up to 150% on the first sampling date, 24 May 2012. MFM declined steadily until mid-August as drought developed and FAW dropped. Minimum measured MFM for 2012 was 25% on 14 August (Fig. 3e). In 2013, MFM started out in May with similar values to those in 2012, but MFM increased in late May and June, reaching maximum values near 200%. Subsequently, MFM dropped slightly and stabilised at ~100% late June through August. Then, MFM declined further in September 2013, reaching minimum levels at ~50% at the same time that FAW fell to <0.2. The MFM levels did not increase in October, despite increased soil moisture availability.

In 2012, DFM was low all growing season, mostly in the range of 0–20% with values <10% for a large portion of the season (Fig. 3g). In 2013, DFM values were slightly higher than in 2012, mostly in the range from 5 to 30% (Fig. 3h). After the prescribed burn on 15 October 2012 (Patches 3), measurable dead fuel loads were not observed in those patches until late August 2013. The range of DFM was much smaller than that of MFM or GFM.

Relationships between FAW and fuel moisture

The dynamic fuel model of Scott and Burgan (2005) categorises herbaceous fuels based on moisture content, with live herbaceous moisture >120% indicating ‘uncured’ fuels, live herbaceous moisture >30% and ≤120% indicating ‘partially cured’ fuels, and herbaceous moisture ≤30% indicating ‘fully cured’ fuels. The 0–30% moisture category is also used in McArthur’s Mk 5 fire danger meter Grassland Fire Danger Index (GFDI) (Noble *et al.* 1980) and represents herbaceous fuel moisture values (MFM) above which fire will not spread (30% moisture of extinction) (Cruz *et al.* 2015a). We grouped our fuel moisture observations according to these thresholds to determine the soil moisture (FAW) conditions associated with each and present the results in the form of box plots (Fig. 4). Statistically significant differences existed between median FAW levels across fuel moisture categories and are indicated by non-overlapping notches in the box plots. GFM values were typically >120%, and when these high GFM values occurred, FAW values spanned across essentially the entire observed range of values (Fig. 4). However, GFM values sometimes dropped below 120% during dry conditions, and when GFM was <120%, FAW values were nearly always <0.5. GFM values were never <30%.

In contrast to GFM, when MFM values were >120%, FAW values did not span the entire observed range but instead were typically >0.6 (Fig. 4). When MFM was between 30% and 120%, FAW values spanned a wide range but were typically between 0.3 and 0.6. When MFM values dropped below 30%,

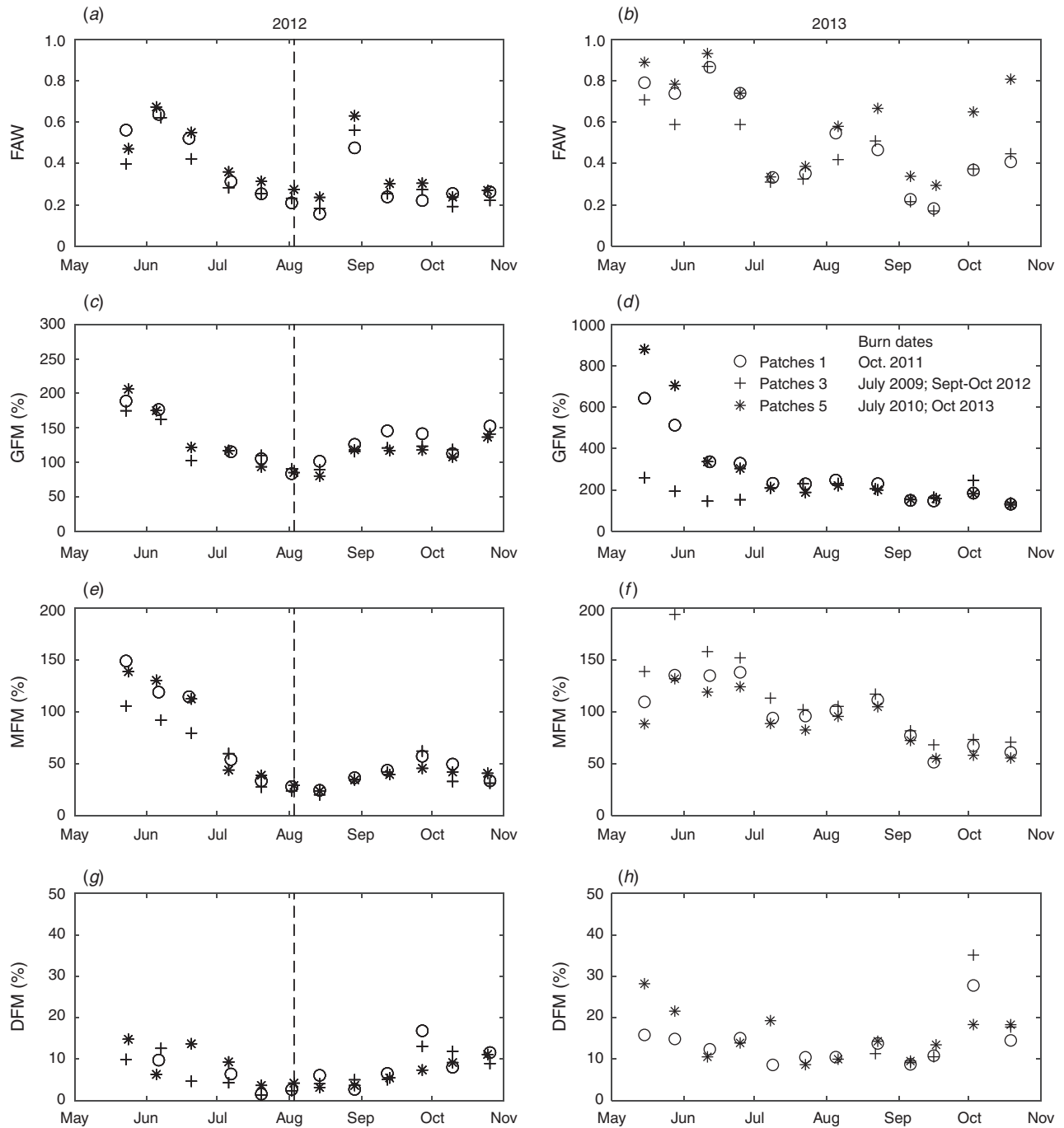


Fig. 3. Time series of fraction of available water capacity (FAW) for the 0–40-cm layer, green fuel moisture (GFM), fuel moisture of the mixed live and dead herbaceous fuels (MFM), and dead fuel moisture (DFM), grouped by burn date (the date the sampled patch was burned) for the 2012 and 2013 growing seasons. Each data point is the mean across three patches, which share the same burn dates. The dashed vertical line marks 3 August 2012, the start of a large wildfire outbreak in Payne County, Oklahoma, the county in which these data were collected. Wildfires burned >34 600 ha in the vicinity of the research site during 2–5 August 2012.

FAW values were always less than 0.3. DFM was nearly always <30% and apparently unrelated to FAW. This dependence of MFM on FAW was quantified using piecewise linear regression (Fig. 5), and we found that below a threshold of FAW = 0.59, MFM significantly decreased with decreasing FAW ($r^2 = 0.74$).

Influence of FAW on the rate and degree of herbaceous fuel curing

Likewise, piecewise linear regression showed a strong and inverse linear relationship between herbaceous fuel curing rate and FAW for FAW values ≤ 0.3 ($r^2 = 0.79$, Fig. 6). The curing

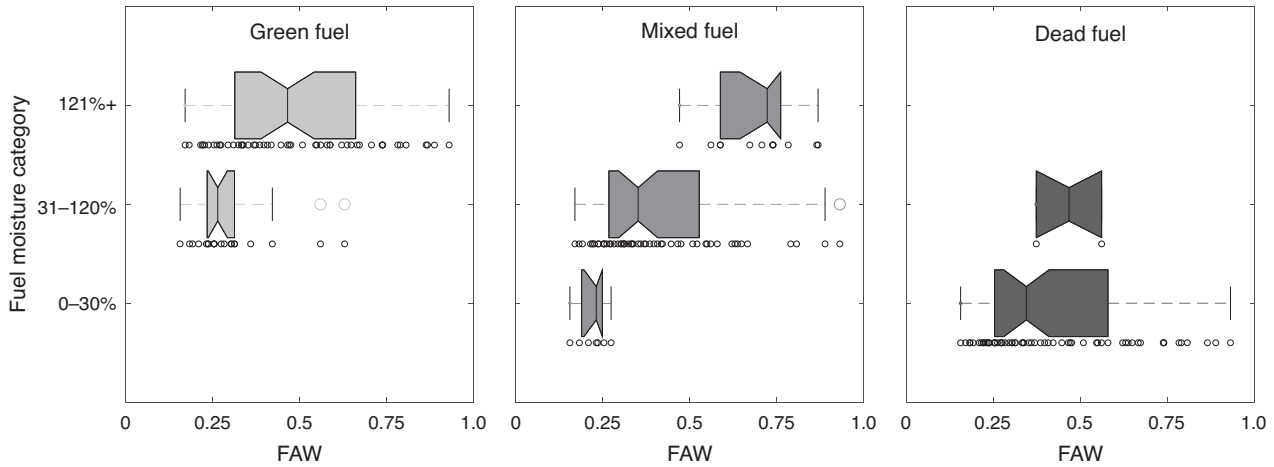


Fig. 4. Soil moisture, expressed as fraction of available water capacity (FAW) measured for the 0–40-cm soil layer, v. concurrent fuel moisture values grouped in the three fuel moisture categories of Scott and Burgan (2005) for green fuel moisture (GFM), fuel moisture of the mixed live and dead herbaceous fuels (MFM), and dead fuel moisture (DFM). All data were collected during the 2012 and 2013 growing seasons in tallgrass prairie in Oklahoma. Median lines are the black lines near the middle of each box, the 25th and 75th percentile values are the left and right sides of boxes, the whiskers indicate the range of data, and the outliers are represented as individual points outside of the whiskers. The individual FAW values are also shown as circles beneath each box to display details of data distribution.

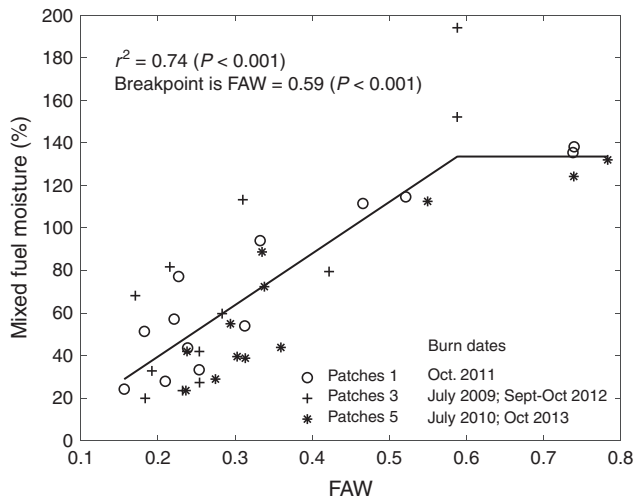


Fig. 5. Mixed-fuel moisture v. fraction of available water capacity (FAW) for the 0–40-cm soil layer for sampling intervals during the growing season when the soil moisture was declining. The coefficient of determination (r^2) and breakpoint were identified using piecewise linear regression.

rate in this context is the rate at which fuels transition from live (i.e. green or partially cured) to dead (i.e. totally cured). The maximum observed curing rate was $12.6 \text{ g m}^{-2} \text{ d}^{-1}$ averaged over the period 6–16 September 2013, a period when FAW averaged 0.21. The curing rate was near zero when FAW values were >0.3 . For most of the measurement intervals, the uncertainty in the curing rate was low, and the uncertainty did not appreciably impact the form of the relationship between FAW and curing rate.

The measured NDVI values, which are often considered an indication of the degree of curing, displayed a strong logistic relationship with FAW during the time periods when FAW was

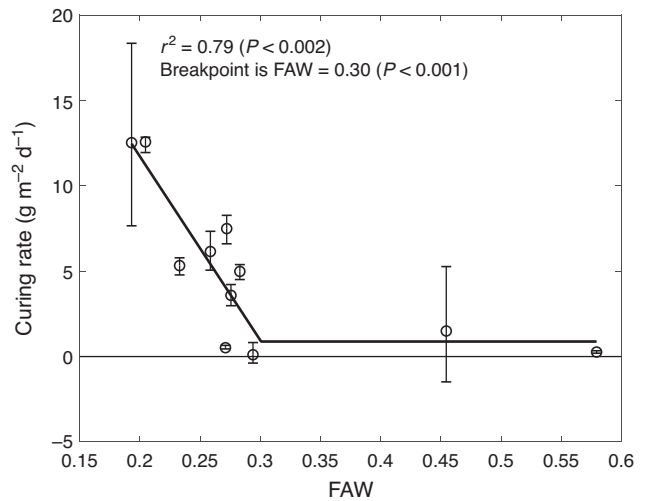


Fig. 6. Estimated curing rate (CR), i.e. rate at which herbaceous fuels transition from live to dead, v. fraction of available water capacity (FAW) for the 0–40-cm soil layer. Circles represent the average CR of the three CR values calculated using LFM₁, LFM₂ and LFM₃. Error bars indicate the uncertainty in the CR estimate due to uncertainty in the true value of live fuel moisture. The r^2 and breakpoint were identified using piecewise linear regression.

declining ($r^2 = 0.83$, Fig. 7). The FAW_{crit} value calculated by Eqn 9 was 0.36, indicating the FAW value below which the decline in NDVI begins, i.e. the fuelbed greenness begins to decrease. If NDVI effectively represents the greenness of the fuelbed, then the inflection point of the curve represents a condition where the fuelbed has lost 50% of its greenness, and this occurred at $\text{FAW} = 0.30$. Four data points measured on 6 and 16 September 2013 were considered outliers and excluded when fitting the logistic equation. These outliers occurred

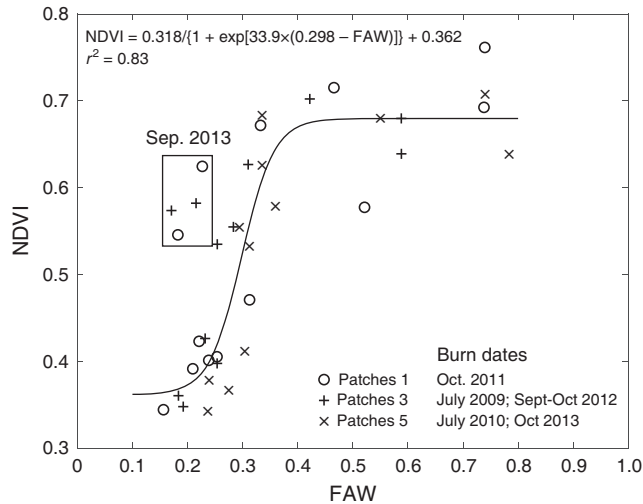


Fig. 7. Normalized Difference Vegetative Index (NDVI) v. fraction of available water capacity (FAW) for the 0–40-cm soil layer for every sampling time in the growing season when the soil moisture was declining, i.e. lower than the prior value. NDVI is a widely used proxy for the degree of fuelbed curing. Each data point is the mean across three patches, which share the same burn dates. The data points inside the rectangle were measured 6 and 16 September 2013, and were considered outliers for reasons explained in the text. The best-fit logistic equation, excluding these data, and the associated r^2 are displayed in the graph.

following a period of rapid FAW decline from 23 August to 6 September, which dropped FAW from more than 0.4 to near 0.2 in two of the burning treatments (Patches 1 and 3, Fig. 3b). This sudden decline of FAW accompanied a simultaneous decline in GFM and MFM (Fig. 3d, f) and led to the greatest observed curing rate (Fig. 6), but NDVI values failed to reflect these important fuelbed changes.

Discussion

This study quantifies the relationships between soil moisture, as represented by FAW, and grassland fuel moisture, CR and greenness during the growing season. We found that declines in soil moisture correspond predictably with declines in grassland fuel moisture, and below specific threshold values, FAW is strongly related to fuel moisture (for $FAW < 0.59$), vegetation greenness as reflected by NDVI (for $FAW < 0.36$) and CR (for $FAW < 0.30$). Although soil moisture has been empirically linked to wildfire probability and size at regional (Krueger *et al.* 2015, 2016, 2017), national (Jensen *et al.* 2018) and global scales (O *et al.* 2020), our results provide a mechanistic explanation for these empirical relationships. Furthermore, because FAW may be more amenable to automated, *in situ* monitoring than is fuel moisture itself, our results also suggest that fire danger rating and dynamic fuel models may be improved by incorporating soil moisture information.

Weather conditions and fuel moisture

The contrasting weather patterns of severe drought in 2012 and near-average weather conditions in 2013 provided an ideal environment for studying the relationships between soil

moisture and grassland fuelbed characteristics. The precipitation deficits in the summer of 2012 resulted in a rapid-onset (flash) drought, which was reflected in measured soil moisture at Oklahoma Mesonet stations across central and eastern Oklahoma (Ford *et al.* 2015), with statewide average FAW values near 0.2 in July and August 2012 (Krueger *et al.* 2015). The drought conditions in 2012 led to major growing-season wildfire outbreaks, which burned an estimated area of 93 043 ha across the state (Krueger *et al.* 2015).

GFM showed phenologically driven decline from the start to the end of the growing season. High moisture content of the tissues produced in early vegetative growth gives way to lower moisture content as the tissues mature. Maximum GFM values in this study are high relative to values reported in previous studies. For example, during one season for two grasslands in Victoria, Australia, GFM values ranged between 65 and 213% (Kidnie *et al.* 2015). The GFM values $>400\%$ that we recorded in May 2013 could conceivably be the result of dew or rainfall on vegetation or other sampling errors, but no clear evidence for such errors was identified in a review of all related field notes and data files; thus, these values could not justifiably be removed. Although these GFM values exceed typical fuel moisture values for grasses, they were within the range of GFM values for some forb species. For example, Polley *et al.* (2020) report leaf dry matter content values as low as 12% for forbs in grasslands in Texas, USA, which is equivalent to GFM values as high as 740%. Thus, the high GFM values in May 2013 could be due to high FAW values, coupled with inadvertent preferential sampling of forb species.

The fuel moisture of the mixed live and dead herbaceous fuels (MFM) observed here is comparable with typical grassland LFM values in the literature. For example, LFM in guinea grass-dominated sites in Hawaii, USA, ranged from 50 to 300% (Ellsworth *et al.* 2017), which is comparable with the range of MFM in our study (20–200%). Similarly, fuel moisture of mixed live and dead herbaceous materials from grassland in Spain ranged from 10 to 250% (Chuvienco *et al.* 2004), in Germany, it ranged from 20 to 300% (Wittich 2011), and in California, USA, from 6 to 304% (Livingston and Varner 2016). Although MFM and LFM are closely related, there may be good reasons to prefer MFM over LFM for characterisation of herbaceous fuels in grassland.

Because live fuel includes both pure green and senescing fuels (Kidnie *et al.* 2015), measuring LFM raises conceptual and practical problems. How precisely does one determine when a senescing portion of a leaf or stem is no longer live but dead? How much time is needed to completely separate live from dead fuel in the large number of fuelbed samples that is typically required to represent a single grassland patch or pasture? With that level of time commitment, how can one effectively measure changes over time to inform dynamic fuelbed models? Additionally, how can one ensure that different people classify and separate live and dead fuels in the same way? Perhaps most importantly, why is it necessary to separately represent live and dead fuel moisture in grassland fuelbeds given the fact that DFM is typically $<30\%$ and exhibits trivial variation relative to that of the total fuelbed (Fig. 3 and Kidnie *et al.* 2015; Ellsworth *et al.* 2017)? Experiments in Australian grasslands have shown that LFM was not significantly related to the damping of the rate of fire advance in grasslands (Pearson correlation

coefficient -0.286 , $P = 0.343$), whereas MFM was significantly related (Pearson correlation coefficient -0.631 , $P = 0.021$) (Cruz *et al.* 2015b). MFM measurements may be more practical and more relevant than LFM measurements for assessing fuel moisture and fire behaviour in grassland fuelbeds.

Soil moisture and fuel moisture

Grassland MFM values corresponding to the categories in the dynamic fuel model of Scott and Burgan (2005) were associated with significantly different FAW values (Fig. 4), suggesting that FAW measurements may play a useful role in the implementation of such models. Growing-season MFM values $<30\%$, corresponding to the fully cured category of Scott and Burgan (2005) and the mixed fuel moisture of extinction described by McArthur (Cruz *et al.* 2015a), occurred only when FAW was <0.3 . Measured MFM values only approached that range once during the study period, during the first 2 weeks of August 2012, when FAW values were near their minimum (Fig. 3). It was precisely at this time the wildfire outbreak occurred. However, although MFM values below 30% occurred only when FAW was <0.3 , the influence of FAW on MFM values began at FAW values as high as 0.59 (Fig. 5). This result suggests that declining soil moisture conditions may provide an early indication of declining MFM values, well before MFM reaches critical levels.

The 2012 wildfire outbreak provided an important demonstration of the potential for using FAW in fire danger ratings. On 3 August 2012, the day the Payne County wildfires began, the measured MFM averaged 27%, with some patches as low as 22%. These critically low MFM values and corresponding wildfires were preceded by average FAW values that first dropped below 0.3 on 20 July 2012, 2 weeks before the fires. The average FAW value at the time of the fires was 0.24. This result is consistent with the fact that 81% of large (≥ 121 ha) growing-season wildfires in Oklahoma occur when FAW is <0.25 (Krueger *et al.* 2017). The data in Figs 3–5 provide strong quantitative support for the mechanistic linkages from low FAW levels to low grassland MFM levels to the occurrence of large wildfires during the growing season.

Soil moisture and curing

FAW shows strong potential as an early-warning indicator for wildfire danger in the growing season. The transfer of live fuel to dead fuel in these grasslands occurred primarily when FAW was <0.3 , and the curing rate was inversely related to FAW in that range (Fig. 6). Cruz *et al.* (2015b) determined that dead fuel loads as low as 70 g m^{-2} could sustain fire propagation in partially cured grasslands. Based on the piecewise linear relationship in Fig. 6, that dead fuel load could be produced in ~ 5.5 days when FAW = 0.2 or 11 days when FAW = 0.25.

If grassland dead fuel loads at the start of the growing season are low, then a period of weeks at FAW <0.3 may be required to accumulate sufficient dead fuel to support a large wildfire in grassland. The longer the period of FAW <0.3 , the greater the cumulative degree of curing, until the fuels are fully cured. Grasslands in Oklahoma often produce 300 g m^{-2} of above-ground biomass during a growing season (Powell *et al.* 1986), which would fully cure in 26 days at FAW = 0.2 given the relationship in Fig. 6. This is consistent with the fact that FAW

fell below ≤ 0.2 on average 29 days before the 10 largest growing-season fires in Oklahoma in the 13-year dataset of Krueger *et al.* (2017).

Our results show that estimates of the degree of curing based on NDVI or similar vegetation indices (e.g. Martin *et al.* 2009; Newnham *et al.* 2011) may obscure the fact that up to 50% loss of fuelbed greenness may occur without any corresponding curing, defined as transition from live to dead fuels. The grassland fuelbeds in the present study showed decreasing greenness when FAW declined below 0.36 (Fig. 7); however, substantial transition from live fuel to dead fuel did not occur until FAW declined below 0.30 (Fig. 6). In fact, this FAW threshold at which the transition from live to dead fuel (i.e. curing) began is identical to the FAW value at which the fuelbed greenness had already decreased by 50% from its maximum value. This result is reasonable given the typical progression of drought effects, with decreased greenness associated with wilting and leaf rolling preceding tissue death. Another distinction between NDVI and FAW is that NDVI can exhibit time lags of 2–4 weeks in response to changing environmental conditions (Wang *et al.* 2010). This lag was evident in our data during September 2013, when rapid FAW decline and high rates of curing were measured but NDVI was relatively unaffected.

The results of this study are generally consistent with a growing body of literature documenting the influence of soil moisture on dynamic fuelbed characteristics. In north-western Sardinia in Italy, soil moisture was more highly correlated with LFM than were weather variables for four Mediterranean shrub species (Pellizzaro *et al.* 2007). Likewise, soil moisture was also more strongly correlated with LFM for shrub species of Gambel oak (*Quercus gambelii* Nutt.) and big sagebrush (*Artemisia tridentata* Nutt.) than was remotely sensed NDVI or Normalized Difference Water Index (NDWI) across 10 sites in northern Utah, USA (Qi *et al.* 2012). Additionally, summertime decreases in soil moisture occurred simultaneously with decreasing greenness and MFM in cool-season grasses in Germany (Wittich 2011).

One key limitation of this study is the mismatch in spatial scale between the soil moisture and vegetation data. Each of the nine patches in this study contained only one soil moisture measurement location but 12 vegetation sampling locations per sampling date. Although soil moisture observations in Oklahoma can be spatially correlated at distances up to 30 km or more (Dong and Ochsner 2018; Ochsner *et al.* 2019), soil moisture is also heterogeneous at scales as small as a few metres (Famiglietti *et al.* 2008). The discrepancy in the spatial scale of our measurements might have reduced the apparent relationship strength between FAW and the fuelbed variables. Despite this limitation, the data proved adequate to reveal the strong connection between FAW and MFM and between FAW and rate of curing in these grassland fuelbeds. These results strongly suggest the use of *in situ* FAW monitoring to signal potentially low grassland fuel moisture conditions, accelerated curing and elevated growing-season fire danger.

Conclusion

Previous studies showed that large growing-season wildfires in Oklahoma occur primarily when the soil moisture metric FAW

drops below 0.2 (Krueger *et al.* 2015), that the probability of wildfire can increase 3-fold as FAW decreases from 0.5 to 0.2 (Krueger *et al.* 2016), and that the association between decreasing soil moisture and wildfire is evident worldwide (O *et al.* 2020), but the mechanism behind these relationships remained speculative. This study addresses this knowledge gap, showing that: (1) declines in grassland MFM occur as FAW values drop below 0.59, and (2) MFM values can drop below 30% and the grassland curing rate increases linearly as FAW drops below 0.30, thereby increasing wildfire danger. Furthermore, when FAW reaches ~ 0.20 , a recommended threshold for extreme wildfire danger, grassland live to dead fuel transition can reach rates $> 10 \text{ g m}^{-2} \text{ d}^{-1}$.

As soil moisture data become increasingly available owing to the development of *in situ* monitoring networks and soil moisture satellites, the prospect of using soil moisture data in growing-season fire danger assessments becomes increasingly attractive. In fact, FAW maps have recently been added to OK-FIRE (<https://www.mesonet.org/index.php/okfire>; accessed 24 September 2020), a decision-support system used by thousands, including wildland fire managers and the public in Oklahoma, USA (Joint Fire Science Program 2011). In the future, estimating MFM and CRs for herbaceous fuels based on observed FAW could contribute to better dynamic representations of fuelbed parameters in fire danger models for similar grassland ecosystems around the world. The resulting improvements in growing-season fire danger ratings could enhance wildfire preparedness and response, which could help reduce the devastating impacts of wildfire on property and lives.

Conflicts of interest

The authors declare no conflicts of interest.

Acknowledgements

Funding for this project was provided by the Joint Fire Science Program Grant no. 11–1–2–19, the South-Central Climate Adaptation Science Center grants no. G15AP00151 and G18AC00278, and USDA National Institute of Food and Agriculture Hatch Project OKL02918, and the Division of Agricultural Sciences and Natural Resources at Oklahoma State University. Oklahoma Mesonet data are provided courtesy of the Oklahoma Mesonet, which is jointly operated by Oklahoma State University and the University of Oklahoma. Continued funding for maintenance of the network is provided by the taxpayers of Oklahoma. The authors thank Chris Stansberry, Superintendent of the Oklahoma State University Range Research Station, and John Weir, Associate Extension Specialist for Prescribed Fire, for maintaining the long-term patch burn experiment.

References

- Allan G, Johnson A, Cridland S, Fitzgerald N (2003) Application of NDVI for predicting fuel curing at landscape scales in northern Australia: can remotely sensed data help schedule fire management operations? *International Journal of Wildland Fire* **12**, 299–308. doi:10.1071/WF03016
- Allen RG, Pereira LS, Raes D, Smith M (1998) Crop evapotranspiration – Guidelines for computing crop water requirements. FAO Irrigation and Drainage paper 56. (FAO: Rome, Italy) 300 pp.
- Bielski CH, Twidwell D, Fuhlendorf SD, Wonkka CL, Allred BW, Ochsner TE, Krueger ES, Carlson JD, Engle DM (2018) Pyric herbivory, scales of heterogeneity and drought. *Functional Ecology* **32**, 1599–1608. doi:10.1111/1365-2435.13083
- Chen HI, Chang K-C (1991) Assessment of threshold and saturation pressure in the baroreflex function curve: a new mathematical analysis. *Japanese Journal of Physiology* **41**, 861–877. doi:10.2170/JJPHYSIOL.41.861
- Cheney NP, Gould JS, Catchpole WR (1998) Prediction of fire spread in grasslands. *International Journal of Wildland Fire* **8**, 1–13. doi:10.1071/WF980001
- Chuvieco E, Cocero D, Riano D, Martin P, Martinez-Vega J, de la Riva J, Perez F (2004) Combining NDVI and surface temperature for the estimation of live fuel moisture content in forest fire danger rating. *Remote Sensing of Environment* **92**, 322–331. doi:10.1016/J.RSE.2004.01.019
- Cooper C, Hyder D, Petersen R, Sneva F (1957) The constituent differential method of estimating species composition in mixed hay. *Agronomy Journal* **49**, 190–193. doi:10.2134/AGRONJ1957.00021962004900040007X
- Cruz M, Gould J, Alexander M, Sullivan A, McCaw W, Matthews S (2015a) ‘A guide to rate of fire spread models for Australian vegetation.’ (CSIRO Land and Water: Canberra, ACT, and AFAC: Melbourne, Vic., Australia)
- Cruz MG, Gould JS, Kidnie S, Bessell R, Nichols D, Slijepcevic A (2015b) Effects of curing on grassfires: II. Effect of grass senescence on the rate of fire spread. *International Journal of Wildland Fire* **24**, 838–848. doi:10.1071/WF14146
- Deák B, Valkó O, Török P, Végvári Z, Hartel T, Schmotzer A, Kapocsi I, Tóthmérész B (2014) Grassland fires in Hungary – experiences of nature conservationists on the effects of fire on biodiversity. *Applied Ecology and Environmental Research* **12**, 267–283. doi:10.15666/AEER/1201_267283
- Dennison PE, Moritz MA, Taylor RS (2008) Evaluating predictive models of critical live fuel moisture in the Santa Monica Mountains, California. *International Journal of Wildland Fire* **17**, 18–27. doi:10.1071/WF07017
- Dong J, Ochsner TE (2018) Soil texture often exerts a stronger influence than precipitation on mesoscale soil moisture patterns. *Water Resources Research* **54**, 2199–2211. doi:10.1002/2017WR021692
- Ellsworth LM, Dale AP, Litton CM, Miura T (2017) Improved fuel moisture prediction in non-native tropical *Megathyrus maximus* grasslands using Moderate-Resolution Imaging Spectroradiometer (MODIS)-derived vegetation indices. *International Journal of Wildland Fire* **26**, 384–392. doi:10.1071/WF16131
- Famiglietti JS, Ryu D, Berg AA, Rodell M, Jackson TJ (2008) Field observations of soil moisture variability across scales. *Water Resources Research* **44**, W01423. doi:10.1029/2006WR005804
- Ford TW, McRoberts DB, Quiring SM, Hall RE (2015) On the utility of *in situ* soil moisture observations for flash drought early warning in Oklahoma, USA. *Geophysical Research Letters* **42**, 9790–9798. doi:10.1002/2015GL066600
- Fuhlendorf SD, Engle D (2004) Application of the fire–grazing interaction to restore a shifting mosaic on tallgrass prairie. *Journal of Applied Ecology* **41**, 604–614. doi:10.1111/J.0021-8901.2004.00937.X
- García M, Chuvieco E, Nieto H, Aguado I (2008) Combining AVHRR and meteorological data for estimating live fuel moisture content. *Remote Sensing of Environment* **112**, 3618–3627. doi:10.1016/J.RSE.2008.05.002
- Gillen RL, Tate KW (1993) The constituent differential method for determining live and dead herbage. *Journal of Range Management* **46**, 142–147. doi:10.2307/4002271
- Gillen RL, McCollum FT, Brummer JE (1990) Tiller defoliation patterns under short duration grazing in tallgrass prairie. *Journal of Range Management* **43**, 95–99. doi:10.2307/3899023
- Jensen D, Reager JT, Zajic B, Rousseau N, Rodell M, Hinkley E (2018) The sensitivity of US wildfire occurrence to pre-season soil moisture conditions across ecosystems. *Environmental Research Letters* **13**, 014021. doi:10.1088/1748-9326/AA9853

- Joint Fire Science Program (2011) OK-FIRE: weather-based decision support for wildland fire management. Fire Science Brief, Issue 127. Available at <https://digitalcommons.unl.edu/jfspbriefs/102/> [Verified 24 September 2020]
- Kidnie S, Cruz MG, Gould J, Nichols D, Anderson W, Bessell R (2015) Effects of curing on grassfires: I. Fuel dynamics in a senescing grassland. *International Journal of Wildland Fire* **24**, 828–837. doi:10.1071/WF14145
- Krueger ES, Ochsner TE, Engle DM, Carlson J, Twidwell D, Fuhlendorf SD (2015) Soil moisture affects growing-season wildfire size in the Southern Great Plains. *Soil Science Society of America Journal* **79**, 1567–1576. doi:10.2136/SSSAJ2015.01.0041
- Krueger ES, Ochsner TE, Carlson J, Engle DM, Twidwell D, Fuhlendorf SD (2016) Concurrent and antecedent soil moisture relate positively or negatively to probability of large wildfires depending on season. *International Journal of Wildland Fire* **25**, 657–668. doi:10.1071/WF15104
- Krueger ES, Ochsner TE, Quiring SM, Engle DM, Carlson J, Twidwell D, Fuhlendorf SD (2017) Measured soil moisture is a better predictor of large growing-season wildfires than the Keetch–Byram Drought Index. *Soil Science Society of America Journal* **81**, 490–502. doi:10.2136/SSSAJ2017.01.0003
- Limb RF, Fuhlendorf SD, Engle DM, Weir JR, Elmore RD, Bidwell TG (2011) Pyric–herbivory and cattle performance in grassland ecosystems. *Rangeland Ecology and Management* **64**, 659–663. doi:10.2111/REM-D-10-00192.1
- Linn R, Reisner J, Colman JJ, Winterkamp J (2002) Studying wildfire behavior using FIRETEC. *International Journal of Wildland Fire* **11**, 233–246. doi:10.1071/WF02007
- Livingston AC, Varner JM (2016) Fuel moisture differences in a mixed native and non-native grassland: implications for fire regimes. *Fire Ecology* **12**, 73–87. doi:10.4996/FIREECOLOGY.1201073
- Marino E, Dupuy J-L, Pimont F, Guijarro M, Hernando C, Linn R (2012) Fuel bulk density and fuel moisture content effects on fire rate of spread: a comparison between FIRETEC model predictions and experimental results in shrub fuels. *Journal of Fire Sciences* **30**, 277–299. doi:10.1177/0734904111434286
- Martin D, Grant I, Jones S, Anderson S (2009) Development of satellite vegetation indices to assess grassland curing across Australia and New Zealand. In ‘Innovations in remote sensing and photogrammetry’. (Eds S Jones, K Reinke) pp. 211–227. (Springer-Verlag: Berlin, Germany)
- Mathworks (2018) ‘Matlab version R2018a for Windows.’ (The MathWorks Inc.: Natick, MA, USA)
- McPherson RA, Fiebrich CA, Crawford KC, Kilby JR, Grimsley DL, Martinez JE, Basara JB, Illston BG, Morris DA, Kloesel KA (2007) Statewide monitoring of the mesoscale environment: a technical update on the Oklahoma Mesonet. *Journal of Atmospheric and Oceanic Technology* **24**, 301–321. doi:10.1175/JTECH1976.1
- Mell WE, Manzello SL, Maranghides A, Butry D, Rehm RG (2010) The wildland–urban interface fire problem – current approaches and research needs. *International Journal of Wildland Fire* **19**, 238–251. doi:10.1071/WF07131
- Mouillot F, Field CB (2005) Fire history and the global carbon budget: a 1 × 1 fire history reconstruction for the 20th century. *Global Change Biology* **11**, 398–420.
- National Interagency Fire Center (2017) Wildland fire statistics. National Interagency Fire Center. (Boise, ID, USA). Available at http://www.nifc.gov/fireInfo/fireInfo_statistics.html [Verified 17 July 2017]
- Newnham GJ, Verbesselt J, Grant IF, Anderson SAJ (2011) Relative Greenness Index for assessing curing of grassland fuel. *Remote Sensing of Environment* **115**, 1456–1463. doi:10.1016/j.rse.2011.02.005
- Noble IR, Gill AM, Bary GAV (1980) McArthur’s fire-danger meters expressed as equations. *Australian Journal of Ecology* **5**, 201–203. doi:10.1111/j.1442-9993.1980.tb01243.x
- O S, Hou X, Orth R (2020) Observational evidence of wildfire-promoting soil moisture anomalies. *Scientific Reports* **10**, 11008. doi:10.1038/S41598-020-67530-4
- Ochsner TE, Cosh MH, Cuenca RH, Dorigo WA, Draper CS, Hagimoto Y, Kerr YH, Njoku EG, Small EE, Zreda M (2013) State of the art in large-scale soil moisture monitoring. *Soil Science Society of America Journal* **77**, 1888–1919. doi:10.2136/SSSAJ2013.03.0093
- Ochsner TE, Linde E, Haffner M, Dong J (2019) Mesoscale soil moisture patterns revealed using a sparse *in situ* network and regression kriging. *Water Resources Research* **55**, 4785–4800. doi:10.1029/2018WR024535
- Overholt KJ, Cabrera J, Kurzwaski A, Koopersmith M, Ezekoye OA (2014) Characterization of fuel properties and fire spread rates for little bluestem grass. *Fire Technology* **50**, 9–38. doi:10.1007/S10694-012-0266-9
- Pellizzaro G, Cesaraccio C, Duce P, Ventura A, Zara P (2007) Relationships between seasonal patterns of live fuel moisture and meteorological drought indices for Mediterranean shrubland species. *International Journal of Wildland Fire* **16**, 232–241. doi:10.1071/WF06081
- Polley WH, Yang C, Wilsey BJ, Fay PA (2020) Spectrally derived values of community leaf dry matter content link shifts in grassland composition with change in biomass production. *Remote Sensing in Ecology and Conservation*. doi:10.1002/RSE2.145
- Powell J, Stadler S, Claypool P (1986) Weather factors affecting 22 years of tallgrass prairie hay production and quality. *Journal of Range Management* **39**, 354–361. doi:10.2307/3899779
- Qi Y, Dennison P, Spencer J, Riaño D (2012) Monitoring live fuel moisture using soil moisture and remote sensing proxies. *Fire Ecology* **8**, 71–87. doi:10.4996/FIREECOLOGY.0803071
- Rothermel RC (1972) A mathematical model for predicting fire spread in wildland fuels. USDA Forest Service, Intermountain Forest and Range Experiment Station, Research Paper INT-RP-115. (Ogden, UT, USA)
- Rouse J, Haas R, Schell J, Deering D (1974) Monitoring vegetation systems in the Great Plains with ERTS. *NASA Special Publication* **351**, 309–317.
- Scott JH, Burgan RE (2005) Standard fire behavior fuel models: a comprehensive set for use with Rothermel’s surface fire spread model. USDA Forest Service, Rocky Mountain Research Station, Research Paper RMRS-GTR-153, pp. 1–72. (Fort Collins, CO, USA)
- Seber GAF, Wild CJ (2003) ‘Non-linear regression.’ (Wiley-Interscience: Hoboken, NJ, USA)
- Sharma S, Ochsner TE, Twidwell D, Carlson J, Krueger ES, Engle DM, Fuhlendorf SD (2018) Non-destructive estimation of standing crop and fuel moisture content in tallgrass prairie. *Rangeland Ecology and Management* **71**, 356–362. doi:10.1016/j.rama.2018.01.001
- Sridhar V, Hubbard KG, You J, Hunt ED (2008) Development of the soil moisture index to quantify agricultural drought and its ‘user friendliness’ in severity–area–duration assessment. *Journal of Hydrometeorology* **9**, 660–676. doi:10.1175/2007JHM892.1
- Twidwell D, West AS, Hiatt WB, Ramirez AL, Winter JT, Engle DM, Fuhlendorf SD, Carlson J (2016) Plant invasions or fire policy: which has altered fire behavior more in tallgrass prairie? *Ecosystems* **19**, 356–368. doi:10.1007/S10021-015-9937-Y
- Wang J, Rich PM, Price KP (2010) Temporal responses of NDVI to precipitation and temperature in the central Great Plains, USA. *International Journal of Remote Sensing* **22**, 2345–2364.
- Wittich K-P (2011) Phenological observations of grass curing in Germany. *International Journal of Biometeorology* **55**, 313–318. doi:10.1007/S00484-010-0338-9
- Wotton BM, Alexander ME, Taylor SW (2009) Updates and revisions to the 1992 Canadian forest fire behavior prediction system. Canadian Forest Service, Great Lakes Forestry Centre, Information Report GLC-X-10. (Sault Ste Marie, ON, Canada)

- Yebra M, Chuvieco E, Riaño D (2008) Estimation of live fuel moisture content from MODIS images for fire risk assessment. *Agricultural and Forest Meteorology* **148**, 523–536. doi:[10.1016/J.AGRFORMET.2007.12.005](https://doi.org/10.1016/J.AGRFORMET.2007.12.005)
- Yebra M, Dennison PE, Chuvieco E, Riaño D, Zylstra P, Hunt ER, Danson FM, Qi Y, Jurdao S (2013) A global review of remote sensing of live fuel moisture content for fire danger assessment: moving towards operational products. *Remote Sensing of Environment* **136**, 455–468. doi:[10.1016/J.RSE.2013.05.029](https://doi.org/10.1016/J.RSE.2013.05.029)
- Zhang J, Kenworthy K, Unruh JB, Poudel B, Erickson JE, Rowland D, Kruse J (2017) Physiological responses to soil drying by warm-season turfgrass species. *Crop Science* **57**, S-111–S-118. doi:[10.2135/CROPSCI2016.05.0316](https://doi.org/10.2135/CROPSCI2016.05.0316)